

## Development of pH-Responsive Fluorescent False Neurotransmitters

Minhee Lee,<sup>†</sup> Niko G. Gubernator,<sup>‡</sup> David Sulzer,<sup>\*,§</sup> and Dalibor Sames<sup>\*,†</sup>

Department of Chemistry, Columbia University, 3000 Broadway, New York, New York 10027, eMolecules, San Diego, California 92014, and Departments of Neurology, Psychiatry, and Pharmacology, Columbia University Medical Center, New York, New York 10032

Received March 12, 2010; E-mail: ds43@columbia.edu; sames@chem.columbia.edu

As part of a broad program aimed at optical imaging of metabolic and signaling enzymes in cells and tissues,<sup>1,2</sup> we became interested in visualization of neurotransmission. Recently we have introduced fluorescent false neurotransmitters (FFNs), probes that act as optical tracers that provide the first means to image neurotransmitter release from individual presynaptic terminals in the brain.<sup>3</sup> We here report the development of pH-responsive FFNs and demonstrate optical *in situ* measurement of pH and its changes in catecholamine secretory vesicles of intact PC-12 cells.<sup>4</sup>

Monoamine neurotransmitters are accumulated in synaptic vesicles by vesicular monoamine transporter 2 (VMAT2), which translocates the monoamines (e.g., dopamine) from cytosol to the lumen of synaptic vesicles.<sup>5</sup> Similarly, in chromaffin cells of adrenal medulla, epinephrine and norepinephrine are accumulated in secretory vesicles by a closely related protein, VMAT1 (Figure 1). The vesicular lumen is acidic (pH 5–6) due to the action of vacuolar-H<sup>+</sup> ATPase, which imports H<sup>+</sup> at the expense of ATP hydrolysis. The pH gradient between the cytoplasm and the vesicular lumen in turn provides the driving force for the accumulation of transmitters in the vesicles. Thus *the pH gradient is a key parameter regulating synaptic plasticity* as it controls the vesicular transmitter content and amount of transmitter released during vesicle fusion. The pH gradient between the cytosol and the vesicular lumen is ATP-dependent and thus closely coupled to the metabolic state of the presynaptic terminals. Despite the importance of this parameter and great efforts focused on development of fluorescent pH indicators,<sup>6</sup> there are currently no small molecule probes available for selective measurement of pH in synaptic or secretory vesicles. The pH-sensitive synapto-pHluorin protein can be used to estimate pH in synaptic vesicles of cultured neurons.<sup>7</sup> Alternatively, construction of avidin-chimera proteins allows for anchoring a pH-sensitive fluorescent dye, linked to biotin, to specific organelles including secretory vesicles.<sup>8</sup> These approaches, however, require transfection of the cell culture prior to measurement or generation of transgenic animals for studies with tissue.

Commercially available pH-sensitive dyes (e.g., LysoTracker and LysoSensor)<sup>9</sup> are not suitable for this task as they label other acidic organelles including endosomes and lysosomes,<sup>10</sup> and in the brain they do not label presynaptic terminals. A fixable weak base, known as DAMP (3-(2,4-dinitroanilino)-3'-amino-N-methyldipropylamine), can be used to estimate vesicular pH but requires cell fixation, immunostaining with gold particles, and electron microscopy and thus is unsuitable for intact cells and tissues.<sup>10</sup>

Aware of these limitations, we set out to develop pH-responsive FFNs that would act as VMAT substrates with a built-in ratiometric fluorescent pH sensor. The design of pH-responsive FFNs was modeled on probe FFN511 (Figure 2A);<sup>3</sup> the aminoethyl group was

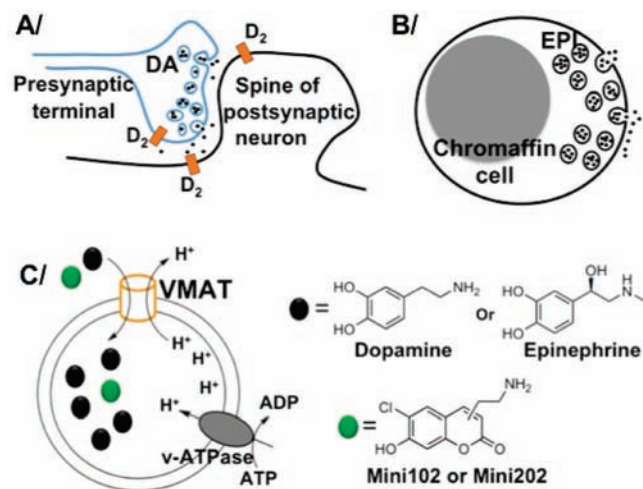


**Figure 1.** Schematic illustration of (A) a dopaminergic presynaptic terminal that modulates the activity of the postsynaptic neuron (DA = dopamine, D2 = dopamine receptor 2). (B) A chromaffin cell in adrenal medulla secreting epinephrine (EPI). (C) Vesicular uptake of endogenous substrates (dopamine or epinephrine) and exogenous fluorescent substrate (e.g., Mini102 or 202) by vesicular monoamine transporter (VMAT).

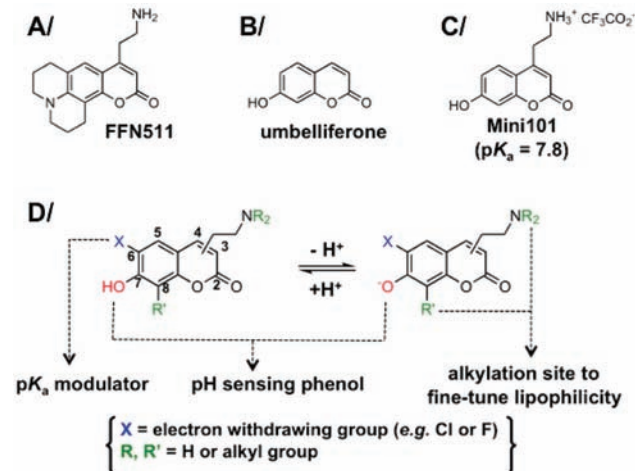


**Figure 2.** Design of pH-responsive FFNs based on the coumarin nucleus. (A) Structure of FFN511, the first example of FFN probes. (B) Structure of umbelliferone. (C) Chemical structure of Mini101. (D) The key structural elements for optimization of photophysical, physical, and functional properties of pH-responsive FFNs.

maintained as the key VMAT recognition element, while the amine in the 7-position of the coumarin nucleus was replaced with the phenol. It is known that phenols exhibit pH-dependent photophysical properties related to the equilibrium between the protonated phenol and the deprotonated phenolate forms. Specifically, 7-hydroxycoumarin (umbelliferone, Figure 2B) exhibits a pH-responsive, ratio-

<sup>†</sup> Columbia University.

<sup>‡</sup> eMolecules.

<sup>§</sup> Columbia University Medical Center.

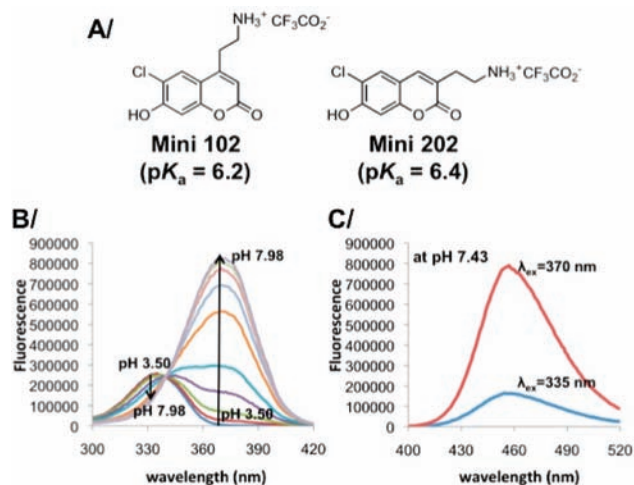


**Figure 3.** (A) Structure of Mini102 and Mini202. (B) Excitation spectra of Mini202 ( $\lambda_{em} = 458$  nm) at different pH values in phosphate buffer. (C) Emission spectra of Mini202 in pH 7.43 phosphate buffer ( $\lambda_{ex} = 335$  and 370 nm, [Mini202] = 2  $\mu$ M).

metric absorption/excitation profile.<sup>11</sup> Accordingly, we synthesized probe Mini101 (Figure 2C), and the  $pK_a$  value of 7.8 was obtained from the absorption measurements. Since the  $pK_a$  of Mini101 is too high for an accurate measurement in the relevant pH range of synaptic or secretory vesicles (5–6), electron-withdrawing groups (Cl and F) were introduced at the 6-position of coumarin to decrease the  $pK_a$  of the phenolic hydroxyl group.

In addition to the photophysical properties, we also aimed to examine the lipophilicity of FFNs as an additional key design parameter that affects membrane permeability by passive diffusion and determines selectivity between VMAT-expressing and nonexpressing cells. Lipophilicity can be fine-tuned by adding alkyl groups to either the coumarin ring (at position C-8) or the amino group (Figure 2D).

According to these design directives, a series of 14 compounds was prepared (see Supporting Information for structure and synthesis). For all compounds, the photophysical properties, pH responsiveness, and lipophilicity were investigated (see Supporting Information). Placing the chlorine or fluorine adjacent to the hydroxy group resulted in a substantial decrease of  $pK_a$ , as exemplified by probes Mini102 and Mini202 (Figure 3A,  $pK_a = 6.2$  and 6.4, respectively). The excitation spectra of the probe Mini202 are shown in Figure 3B; they are strongly dependent on pH, exhibiting two fully resolved maxima at 335 and 370 nm, where the former corresponds to the protonated phenolic form and the latter to the deprotonated phenolate form. Mini202 is sufficiently fluorescent, and the emission intensity ( $\lambda_{max} = 458$  nm) is dependent on the excitation wavelength and pH (Figure 3C). Therefore, the fluorescence intensity ratio at 458 nm obtained by dual excitation at two different wavelengths yields the pH of the solution. In addition, Mini202 is highly polar ( $\log D = -1.5$ , obtained by partitioning between pH 7.4 phosphate buffer and *n*-octanol), which is presumably responsible for slow cell uptake and low background fluorescence (see below).

The compound series was profiled by fluorescence microscopy using human embryonic kidney (HEK) cells stably transfected with VMAT2 (VMAT2-HEK). Six probes showed VMAT2-dependent uptake, with Mini202 displaying the highest uptake at the selected incubation time (Figure 4). VMAT2-HEK cells were incubated with Mini202 (final concn = 20  $\mu$ M) for 30 min and imaged by fluorescence microscopy with  $\lambda_{ex} = 350 \pm 25$  nm and  $\lambda_{em} = 460$

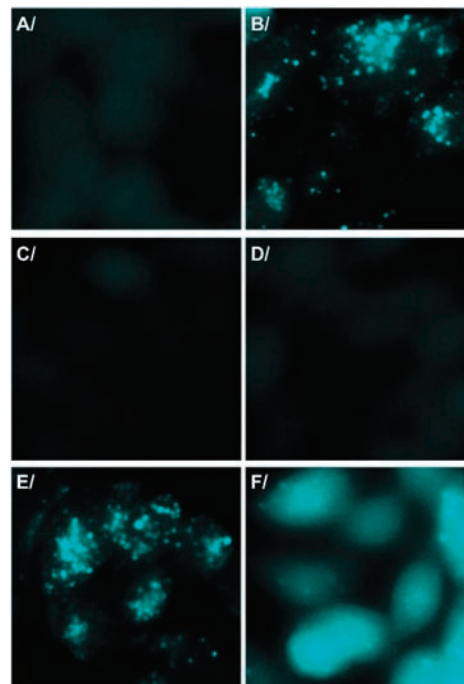


**Figure 4.** Fluorescence microscopy images of Mini202 (20  $\mu$ M, 30 min incubation, all images were taken after rinsing the cells with dye-free media) in (A) nontransfected HEK cells, (B) VMAT2-HEK cells, and (C) VMAT2-HEK cells preincubated with 1  $\mu$ M TBZ or (D) 1  $\mu$ M reserpine. (E) VMAT2-HEK cells labeled with Mini202. (F) The lipophilic base chloroquine (300  $\mu$ M, 3 min) led to redistribution of Mini202 from the acidic vesicles to cytosol.  $\lambda_{ex} = 350 \pm 25$  nm,  $\lambda_{em} = 460 \pm 25$  nm.

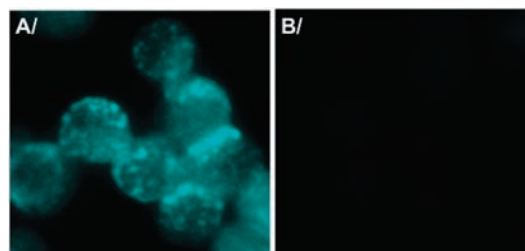


**Figure 5.** (A) PC-12 cells incubated with 20  $\mu$ M Mini202 for 1 h. (B) PC-12 cells preincubated with VMAT1 inhibitor reserpine (1  $\mu$ M, 1 h) followed by 20  $\mu$ M Mini202 treatment for 1 h. The uptake of Mini202 was blocked by reserpine.  $\lambda_{ex} = 350 \pm 25$  nm,  $\lambda_{em} = 460 \pm 25$  nm.

$\pm 25$  nm to afford punctate fluorescence patterns, consistent with VMAT2 expression in acidic organelles (Figure 4B). No uptake of Mini202 was observed in nontransfected HEK cells (Figure 4A), and the uptake of Mini202 was strongly diminished by preincubating VMAT2-HEK cells with the VMAT2 inhibitors, tetrabenazine (TBZ) or reserpine (Figure 4C, 4D). These results indicate that selective accumulation of Mini202 in intracellular organelles is mediated by VMAT2. Furthermore, addition of the lipophilic base chloroquine to the VMAT2-HEK cells labeled with Mini202 resulted in loss of the punctate fluorescent pattern, which is consistent with redistribution of the probes from the vesicles to the cytoplasm caused by collapse of the pH gradient (Figure 4F).

Next, we tested the uptake of Mini202 in PC-12 cells, a cell line derived from a rat pheochromocytoma which is widely used as a model of chromaffin cells and neuronal presynaptic terminals.<sup>4</sup> PC-12 cells express mostly VMAT1 on their secretory large dense core vesicles (LDCVs) where catecholamines accumulate (mostly dopamine and norepinephrine). PC-12 cells were incubated with

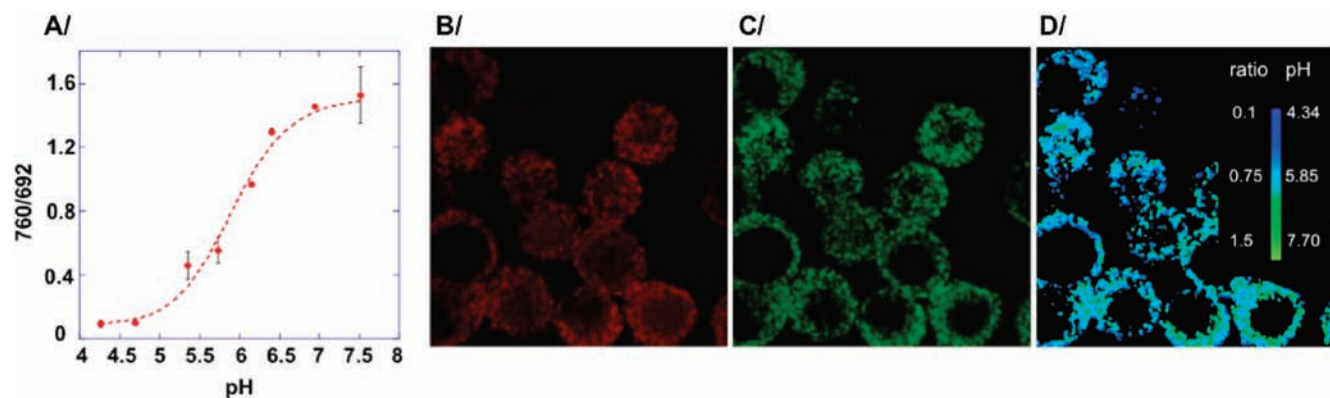


**Figure 6.** Measuring pH of catecholamine secretory vesicles in PC-12 cells with Mini202 via two-photon fluorescence microscopy. (A) *In situ* calibration curve of fluorescence intensity ratio from 760 nm irradiation and 692 nm irradiation ( $\lambda_{em} = 470 \pm 30$  nm,  $pK_a = 5.93 \pm 0.04$ ,  $n = 3$ ) in PC-12 cells as a function of vesicle pH. (B) Two-photon image of PC-12 cells incubated with  $20 \mu\text{M}$  Mini202 for 1 h at  $\lambda_{ex} = 760$  nm and (C)  $\lambda_{ex} = 692$  nm. (D) Pseudocolor image of  $I_{760}/I_{692}$  and corresponding pH values.

Mini202 ( $20 \mu\text{M}$ ) for 1 h and displayed fluorescent puncta consistent with the distribution of LDCVs (Figure 5A). Preincubation of PC-12 cells with VMAT1 inhibitor reserpine ( $1 \mu\text{M}$ ) resulted in no detectable labeling by Mini202 (Figure 5B), indicating that Mini202 labels LDCVs and that Mini202 is a VMAT1 substrate.

Finally, we pursued *in situ* pH measurement of LDCVs in PC-12 cells using a two-photon fluorescence microscope. An *in situ* calibration curve was generated by dual excitation (760 and 692 nm) ratiometric imaging of Mini202 in PC-12 cells, incubated in a series of buffers of known pH in the presence of  $5 \mu\text{M}$  nigericin ( $\text{K}^+/\text{H}^+$  ionophore) and monensin ( $\text{Na}^+/\text{H}^+$  ionophore), which act to equilibrate the vesicular pH with the surrounding media (Figure 6A).<sup>12</sup> Using this calibration curve, the mean pH of LDCVs in PC-12 cells was determined to be  $5.88 \pm 0.08$  by converting the ratio ( $0.75 \pm 0.08$ ) of the two fluorescence intensities obtained from the vesicles after excitation at 760 nm (Figure 6B) and 692 nm (Figure 6C). Although the pH of secretory vesicles has not previously been measured in PC-12 cells, this value is in general agreement with measurements in related cells via *in situ* and other methods (5.4–5.7 in primary chromaffin cells,<sup>10</sup> 5.5 in AtT-20 cells,<sup>8</sup> 5.6–5.7 in synaptic vesicles of hippocampal and dopaminergic neuronal culture<sup>7</sup>).

Furthermore, we quantitatively examined a pharmacological manipulation of vesicular acidity. It has previously been reported that acute exposure of chromaffin cells to methamphetamine rapidly diminishes the pH gradient.<sup>10,13</sup> When PC-12 cells loaded with Mini202 were exposed to  $100 \mu\text{M}$  methamphetamine for 5 min, the emission ratio increased to 1.19, which corresponds to pH 6.36 (Supporting Information, Figure S4). This result is consistent with the proposed pharmacological mode of action of methamphetamine as a transmitter releaser, which at high doses redistributes the vesicular content to the cytoplasm by causing collapse of the pH gradient.

In summary, using rational molecular design, we were able to integrate two molecular functions, the transport by VMAT and ratiometric optical pH sensing, to develop ratiometric pH-responsive FFN probes. Through a systematic effort, Mini202 emerged as the most promising probe, enabling *in situ* pH measurement of catecholamine secretory vesicles and methamphetamine-induced pH changes in PC-12 cells. Mini202 is sufficiently bright, photostable, and suitable for two-photon microscopy. This new agent complements the fluorescent protein tags and may enable the study of mechanisms controlling the secretory pathways in neuroendocrine cells. Also, screening of drugs and other agents for their effects on

pH of secretory vesicles (e.g., transmitter releasing activity or toxicity screens) will be possible. The pH measurement of individual presynaptic terminals in the brain may also be feasible, which is a focus of current studies in our laboratories.

**Acknowledgment.** The authors thank the G. Harold & Leila Y. Mathers Charitable Foundation, the McKnight Foundation, the Picower and Parkinson's Disease Foundations, and NIDA for financial support. We thank Dr. Robert Edwards (UCSF) for providing HEK cells stably transfected with VMAT2 and Dr. Mark Sonders for technical assistance with two-photon microscopy and valuable discussions.

**Supporting Information Available:** The chemical structures, synthetic procedure, structural and photophysical characterization of compounds, and cellular imaging protocols. This material is available free of charge via the Internet at <http://pubs.acs.org>.

## References

- (1) (a) Chen, G.; Yee, D. J.; Gubernator, N. G.; Sames, D. *J. Am. Chem. Soc.* **2005**, *127*, 4544–4545. (b) Halim, M.; Tremblay, M. S.; Jockusch, S.; Turro, N. J.; Sames, D. *J. Am. Chem. Soc.* **2007**, *129*, 7704–7705. (c) Froemming, M. K.; Sames, D. *J. Am. Chem. Soc.* **2007**, *129*, 14518–14522. (d) Tremblay, M. S.; Lee, M.; Sames, D. *Org. Lett.* **2008**, *10*, 5–8. (e) Halim, M.; Yee, D. J.; Sames, D. *J. Am. Chem. Soc.* **2008**, *130*, 14123–14128.
- (2) For examples from other groups: (a) Sharma, V.; Wang, Q.; Lawrence, D. S. *Biochim. Biophys. Acta* **2008**, *1784*, 94–99. (b) Luković, E.; Taylor, E. V.; Imperiali, B. *Angew. Chem., Int. Ed.* **2009**, *48*, 6828–6831. (c) Albers, A. E.; Rawls, K. A.; Chang, C. J. *Chem. Commun.* **2007**, *44*, 4647–4649.
- (3) Gubernator, N. G.; Zhang, H.; Stall, R. G. W.; Mosharov, E. V.; Pereira, D. B.; Yue, M.; Balsanek, V.; Vadola, P. A.; Mukherjee, B.; Edwards, R. H.; Sulzer, D.; Sames, D. *Science* **2009**, *324*, 1441–1444.
- (4) Greene, L. A.; Tischler, A. S. *Proc. Natl. Acad. Sci. U.S.A.* **1976**, *73*, 2424–2428.
- (5) Yelin, R.; Schuldiner, S. *Neurotransmitter Transporters: Structure, Function, and Regulation*, 2nd ed.; Humana Press: Totowa, NJ, 2002; pp 313–354.
- (6) Han, J.; Burgess, K. *Chem. Rev.* **2010**, *110*, 2709–2728.
- (7) (a) Miesenböck, G.; Angelis, D. A. D.; Rothman, J. E. *Nature* **1998**, *394*, 192–195. (b) Mani, M.; Ryan, T. A. *Front. Neural Circuits* **2009**, *3*, 1–9.
- (8) Wu, M. M.; Grabe, M.; Adams, S.; Tsien, R. Y.; Moore, H.-P. H.; Mached, T. E. *J. Biol. Chem.* **2001**, *276*, 33027–33035.
- (9) Haugland, R. P. *The Handbook: A Guide to Fluorescent Probes and Labeling Technologies*, 10th ed.; Invitrogen: Eugene, OR, 2005; pp 937–955.
- (10) Markov, D.; Mosharov, E. V.; Setlik, W.; Gershon, M. D.; Sulzer, D. *J. Neurochem.* **2008**, *107*, 1709–1721.
- (11) Sun, W.-C.; Gee, K. R.; Haugland, R. P. *Bioorg. Med. Chem. Lett.* **1998**, *8*, 3107–3110.
- (12) This is an established method for *in situ* pH calibration of fluorophores in intracellular organelles. For examples: (a) Llopis, J.; McCaffery, J. M.; Miyawaki, A.; Farquhar, M. G.; Tsien, R. Y. *Proc. Natl. Acad. Sci. U.S.A.* **1998**, *95*, 6803–6808. (b) Holopainen, J. M.; Saarikoski, J.; Kinnunen, P. K. J.; Järvelä, I. *Eur. J. Biochem.* **2001**, *268*, 5851–5856.
- (13) Sulzer, D.; Rayport, S. *Neuron* **1990**, *5*, 797–808.

JA101740K